Phys. Med. Biol. **41** (1996) 835–849. Printed in the UK

Photodynamic therapy with pulsed light sources: a theoretical analysis

H J C M Sterenborg and M J C van Gemert

Laser Centre, Academic Medical Centre, University of Amsterdam, Amsterdam, The Netherlands

Received 2 October 1995

Abstract. The effectiveness of photodynamic therapy using pulsed sources was evaluated using a mathematical model describing the time-dependent excitation and de-excitation of the photosensitizer molecule. Using the various numerical data available in the literature on haematoporphyrin we calculated that the effectiveness of pulsed excitation in PDT is identical to that of CW excitation for peak fluence rates below 4×10^8 W m^{-2}. Above this threshold the effectiveness drops significantly. In practice this effect will occur with sources with high pulse energy and low repetition frequency. The commonly used dye lasers pumped by either a Cu vapour laser or a frequency doubled Nd:YAG laser have a PDT effectiveness identical to that of a CW source of the same wavelength and the same average fluence rate.

1. Introduction

A promising new modality for the treatment and diagnosis of superficial cancer is photodynamic therapy (PDT). Although still experimental it is gaining ground rapidly. The technique employs special photosensitizers that concentrate in tumour tissue, some time after administration. The tumour can then be localized by using the fluorescence properties of the photosensitizer. Tumour kill can be obtained by exposing the tissue to (much higher) doses of light. Two pathways of cell killing have been identified. Type I reactions employ the formation of a radical of either oxygen or the photosensitizer molecule. This radical may directly, or indirectly, induce cell damage. In the second pathway, type II reactions, singlet oxygen is generated by the excited photosensitizer molecule. The highly reactive singlet oxygen molecule can be lethal to the cell in which it is formed. The photosensitizer most often clinically in use at present is haematoporphyrin derivative (HpD) or its purified versions Photofrin II® or Photosan®. It is generally assumed that this photosensitizer employs a type II reaction.

In clinical practice the excitation source for therapy is usually a laser. This is mainly for practical reasons: high output in a small wavelength band and the possibility to effectively use optical fibres. The types of laser used vary from CW (argon pumped) dye lasers to pulsed nanosecond (excimer laser pumped) dye lasers. The photodynamic efficacy of pulsed lasers is currently not understood in detail. In principle, a very high peak fluence might saturate the photosensitizer and thus limit the photodynamic effect. Moreover, other tissue chromophores might be saturated, leading to a higher penetration of the light. Laplant *et al* (1987) have shown that with a gold vapour laser such changes in the optical penetration do not occur at average fluence rates of 150 mW cm^{-2}. Several investigators have compared the photodynamic efficacy of pulsed and CW sources. *In vitro* experiments performed by

0031-9155/96/050835+15$19.50

Hasan (1991) showed a marked influence of the pulse duration on the cell killing efficiency. In an *in vivo* experiment by Rausch *et al* (1993) performed in squamous cell carcinomas implanted subcutaneously in nude mice, an excimer pumped dye laser system was shown to be at least as efficient as a CW argon pumped dye laser. A clinical comparison of the pulsed gold vapour laser and the CW argon pumped dye laser for photodynamic therapy of brain tumours performed by Kaye *et al* (1987) showed no significant differences between the efficacy of these two excitation sources. Similar results were obtained by Panjehpur *et al* (1993) comparing the effectiveness of the frequency doubled Nd:YAG (KTP) pumped dye with argon dye in a normal canine oesophagus and by Ferrario *et al* (1991) using a transplanted mammary carcinoma in the rat. The effectiveness of a microsecond flashlamp pumped dye laser was tested by Pope *et al* (1990). The conclusion of this study was that below a fluence of 10^{-2} J cm^{-2} or a fluence rate of 10^4 W cm^{-2} this system is also quite efficient.

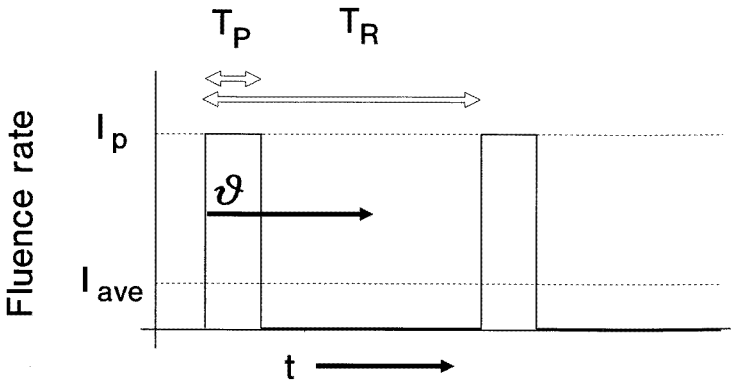

Figure 1. Characteristics of the pulse shape: T_p, pulse duration; T_r, pulse repetition time. The parameter ϑ is a local time variable expressing the time since the start of each pulse.

In this paper we present a mathematical analysis of the effect of pulsed lasers on photosensitizer excitation and singlet oxygen yield. We will make an evaluation of the influence of pulse duration and repetition frequency on the photodynamic effect and make a comparison with CW excitation. In addition, we will determine the conditions needed for saturation and discuss its possible application to PDT.

2. Mathematical model

In this section a mathematical description of the populations of the energy levels involved of the photosensitizer and of oxygen is presented. The model only considers linear absorption; i.e. the absorption probability is proportional to the exciting fluence rate. A biologic damage parameter is defined under the assumption that all damage is singlet oxygen mediated. This biologic damage parameter is used to compare the effectiveness of different excitation sources.

2.1. Light sources

The light source used will be either a CW laser or a pulsed laser. In the case of CW excitation the fluence rate $I(t)$ (W m^{-2}) is given by

$$I(t) = I_0. \tag{1}$$

For a pulsed laser we introduce

$$I(t) = I_p \qquad \text{during the pulse} \tag{2a}$$

$$I(t) = 0 \qquad \text{between pulses.} \tag{2b}$$

Two additional parameters are required to characterize the output of a repetitively pulsed laser: the repetition frequency, f (s^{-1}), and the pulse duration, T_p (s). For convenience, we also introduce the parameter T_r (s), representing the repetition time: $T_r = 1/f$. The average fluence rate, I_{ave}, of the pulsed laser can be calculated from

$$I_{ave} = (T_p/T_r)I_p. \tag{3}$$

The pulse shape and the definitions of the various parameters are illustrated in figure 1.

The fluence rate distribution inside tissue strongly varies in space and depends on the optical absorption and scattering coefficients, as well as the morphology of the tissue. This effect seriously complicates the optical dosimetry of PDT. Presently we will analyse the problem for given fluence rates. Later on we will expand the findings to distributions of fluence rates.

2.2. The photosensitizer

A simplified scheme of the electronic levels of a photosensitizer molecule and the possible paths of excitation and de-excitation are given in figure 2. The levels numbered 0 and 1 refer to the singlet ground state, S_0, and excited state, S_1, respectively and level 2 to the triplet state, T_0. The various possible transitions are indicated by arrows. Spontaneous transition rates (s^{-1}) from state i to state j are denoted by the parameters A_{ij} and k_{ij}, with k referring to radiationless transitions and A to spontaneous transitions in which a photon is emitted. Transition rates of radiation induced transitions are represented by the parameters B (s^{-1} m^2 W^{-1}). It should be noted that all parameters used here are macroscopic parameters that may have units that are slightly different from the more often used single-atom based Einstein parameters. Although high peak fluence rates will be used in the subsequent paragraphs, we will assume linear optics; i.e. the absorption rate is proportional to the local fluence rate, $I(t)$.

Population and depopulation of the three states can be described by the following set of differential equations:

$$\mathrm{d}N_0/\mathrm{d}t = -N_0B_{01}I(t) + N_1(B_{10}I(t) + A_{10} + k_{10}) + N_2(k_{20} + QM_0) \tag{4a}$$

$$\mathrm{d}N_1/\mathrm{d}t = N_0B_{01}I(t) - N_1(B_{10}I(t) + A_{10} + k_{10} + k_{12}) \tag{4b}$$

$$\mathrm{d}N_2/\mathrm{d}t = N_1k_{12} - N_2(k_{20} + QM_0) \tag{4c}$$

where N_0, N_1 and N_2 stand for the population (kmol m^{-3}) of the different states and N_2QM_0 stands for the decrease in the triplet state population by quenching (kmol[1] m^{-3} s^{-1}), a collision induced interaction in which both energy and momentum are transferred from the photosensitizer to an oxygen molecule. Here M_0 is the concentration of ground state oxygen (kmol m^{-3}) and Q the molar quenching rate (kmol^{-1} m^3 s^{-1}). The model presented here does not include photobleaching, the destruction of photosensitizer molecules as a result of

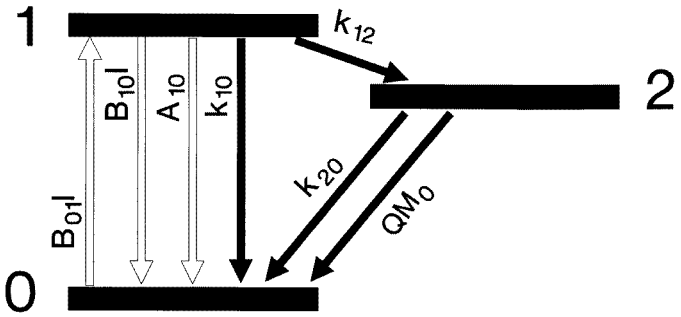

Figure 2. A simplified scheme of the electronic levels of the photosensitizer. Levels 0, 1 and 2 refer to the singlet ground, singlet excited and triplet states, respectively. The various possible transitions are indicated, together with their transition rates. The open arrows refer to radiation related transitions, the solid arrows to radiationless transitions.

irradiation. Thus, $N_0(t) + N_1(t) + N_2(t) = N_0(t = 0)$ at all times. For convenience we introduce the following time constants:

$$\text{the fluorescence decay time} \qquad \tau_f = 1/(A_{10} + k_{10} + k_{12}) \tag{5a}$$

$$\text{the triplet decay time} \qquad \tau_t = 1/[k_{20} + QM_0(t)]. \tag{5b}$$

Moreover, we introduce the following quantum yields:

$$\text{the fluorescence quantum yield} \qquad \Phi_f = A_{10}/(A_{10} + k_{10} + k_{12}) \tag{6a}$$

$$\text{the triplet quantum yield} \qquad \Phi_t = k_{12}/(A_{10} + k_{10} + k_{12}). \tag{6b}$$

2.3. Oxygen

For oxygen we will consider two energy states (figure 3): the triplet ground state, $^3\Sigma_g$, with population M_0; and a singlet excited state, $^1\Delta_g$, with population M_1. Excitation from the $^3\Sigma_g$ ground state to the $^1\Delta_g$ excited state can only occur through quenching of the photosensitizer triplet state. Depopulation of the excited singlet state can take place by two different pathways: by radiative or non-radiative de-excitation to the ground state (α_{10} and κ_{10}) or by an oxidative reaction (κ_{12}). The populations of the two states, M_0 and M_1, are governed by the following set of equations:

$$\mathrm{d}M_0/\mathrm{d}t = -M_0 Q N_2 + M_1(\alpha_{10} + \kappa_{10}) + S \tag{7a}$$

$$\mathrm{d}M_1/\mathrm{d}t = M_0 Q N_2 - M_1(\alpha_{10} + \kappa_{10} + \kappa_{12}) \tag{7b}$$

where α_{10} and κ_{10} represent the singlet to triplet radiative and non-radiative transition rates (s^{-1}) and κ_{12} for the rate at which singlet oxygen is consumed by oxidation reactions and scavengers, and S represents an oxygen supply term (kmol s^{-1}). The latter is a complicated function of perfusion rate and local oxygen gradients. Although the transition from $^1\Delta_g$ to $^3\Sigma_g$ is forbidden it was given a radiative component because luminescence occurring at 1272 nm due to this transition has been observed by many investigators. The singlet oxygen life time,τ_Δ, follows from

$$\tau_\Delta = 1/(\alpha_{10} + \kappa_{10} + \kappa_{12}). \tag{8}$$

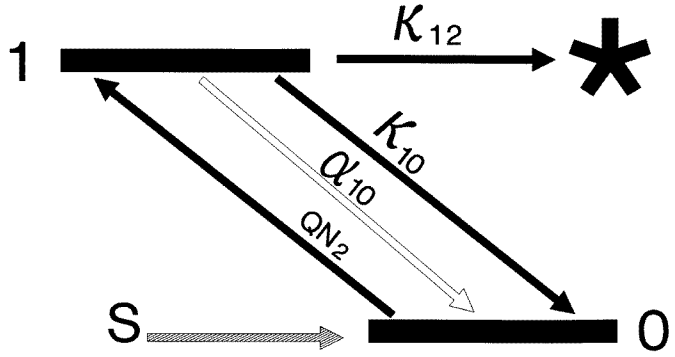

Figure 3. A simplified scheme of the electronic levels of oxygen. Levels 0 and 1 refer to the triplet (ground) state and the singlet (excited) state respectively. For explanation of the arrows and the parameters see the caption of figure 2. The asterisk represents the bound states of oxygen.

2.4. Initial conditions

For CW excitation the initial conditions are given by

$$N_0(t=0) = N_{00} \tag{9a}$$
$$N_1(t=0) = N_2(t=0) = 0 \tag{9b}$$
$$M_0(t=0) = M_{00} \tag{9c}$$
$$M_1(t=0) = 0. \tag{9d}$$

For the case of pulsed excitation we will assume complete relaxation to the ground states to take place before the next excitation pulse arrives. Later on we will show that this is a reasonable assumption for all relevant situations. We can then consider each pulse as a separate event with initial conditions identical to those of the CW case given above. To compress notation we introduce the 'local' time ϑ starting at the beginning of each pulse (figure 1). The initial conditions can now be written as

$$N_0(\vartheta=0) = N_{00} \tag{10a}$$
$$N_1(\vartheta=0) = N_2(\vartheta=0) = 0 \tag{10b}$$
$$M_0(\vartheta=0) = M_{00} \tag{10c}$$
$$M_1(\vartheta=0) = 0. \tag{10d}$$

Solving (4) and (7) for the pulsed case must be done in two steps: first, for $0 < \vartheta < T_p$, i.e. during the pulse using $I(\vartheta) = I_p$ and the initial conditions given in (10). After the pulse, $T_p < \vartheta < T_r$, we take $I(\vartheta) = 0$ and use as initial conditions the populations calculated in the first step for $\vartheta = T_p$:

$$N_0(\vartheta=T_p) = N_0(T_p) \tag{11a}$$
$$N_1(\vartheta=T_p) = N_1(T_p) \tag{11b}$$
$$N_2(\vartheta=T_p) = N_2(T_p) \tag{11c}$$
$$M_0(\vartheta=T_p) = M_0(T_p) \tag{11d}$$
$$M_1(\vartheta=T_p) = M_1(T_p). \tag{11e}$$

2.5. Photodynamic damage

We introduce the photodynamic damage parameter, Ω, expressed as the number of cells per unit volume that dye as a result of the therapy (m^{-3}). We assume that the rate of increase in damage is proportional to the total number of singlet oxygen molecules that is being consumed, i.e. removed from the system:

$$d\Omega(t)/dt = \varepsilon M_1(t)\kappa_{12} \tag{12}$$

where ε ($kmol^{-1}$) is a proportionality constant expressing the sensitivity of the tissue to singlet oxygen, i.e. the number of cells that die per unit volume per kilomole of singlet oxygen. This assumes a pure type II process, i.e. that all biologic damage is singlet oxygen mediated.

The effectiveness of pulsed light, relative to CW light at equal average fluence rate, $I_0 = I_{ave}$, is represented by the dimensionless parameter χ:

$$\begin{aligned}\chi(t) &= \left(\int_t^{t+T_r} \frac{d\Omega_{pulsed}}{dt}\,dt\right) \Big/ \int_t^{t+T_r} \frac{d\Omega_{CW}}{dt}\,dt \\ &= \left(\int_t^{t+T_r} M_{1,pulsed}(t)\,dt\right) \Big/ \int_t^{t+T_r} M_{1,CW}(t)\,dt\end{aligned} \tag{13}$$

where Ω_{pulsed} was calculated with a fluence rate $I_p = I_0 T_r / T_p$. Note that in this definition the parameter $\chi(t)$ is independent of the tissue sensitivity, ε.

3. Numerical values

For the actual values of the different parameters, limited and sometimes contradictory data are available. Moreover, some parameters may depend on the environment and purity of the sample. The numbers used in the present paper refer to haematoporphyrin (HP), as for this photosensitizer the most complete and consistent data set is available. The model presented here, however, is applicable to all photosensitizers, once the relevant rate constants are known.

3.1. The photosensitizer

Fluorescence decay times reported by various authors range from 120 ps to 16 ns. These differences are related to the different aggregates of the photosensitizer molecule and each may vary with concentration and purity. A three-phasic fluorescence decay has been suggested by Schneckenburger *et al* (1988). For the present analysis we shall neglect the short-lived components and use a fluorescence lifetime, τ_f, of 10 ns. This limits the applicability of our results to time scales longer than 10 ns. The sum of the three de-excitation rates, $A_{10} + k_{10} + k_{12}$, which is equal to $1/\tau_f$, must therefore be of the order of 10^{-8} s. At low levels of the excitation fluence rate, the de-excitation from the first excited state occurs by three competing processes, spontaneous emission, internal conversion and inter-system crossing, described by the three parameters A_{10}, k_{10} and k_{12}. The parameter describing the transition from the excited singlet state to the triplet state, k_{12}, can be estimated from the literature values of triplet quantum yield, Φ_t. For HP, a value for Φ_t of 0.71 was reported by Redmond *et al* (1987). Using a fluorescence lifetime $\tau_f = 1/(A_{10}+k_{10}+k_{12})$ of 10^{-8} s we can directly derive from (6*b*) a singlet to triplet transition rate, $k_{12} = 7.1\times10^7\ s^{-1}$. This is close to the value for k_{12} of HP of $10^8\ s^{-1}$ reported by Kozlov *et al* (1987). From this we can derive that $A_{10} + k_{10} = 2.9 \times 10^7\ s^{-1}$, which is the value we will use for

our calculations. Separate values for A_{10} and k_{10} can be calculated from the fluorescence quantum yield measurements. Using the value of Φ_f of 0.066 published by Moan and Sommer (1981), we can derive using (5*a*) $A_{10} = 6.6 \times 10^6$ s^{-1} and $k_{10} = 2.24 \times 10^7$ s^{-1}.

The parameter B_{01} is related to the molar absorption coefficient of the photosensitizer by

$$B_{01} = \mu_{a0}/N_a h\nu \tag{14}$$

where N_a stands for Avogadro's number (kmol^{-1}), $h\nu$ for the phonon energy (J) and μ_{a0} for the molar absorption coefficient (m^2 kmol^{-1}). Bonnet *et al* (1983) reported a value of $\mu_{a0} = 4 \times 10^5$ m^2 kmol^{-1} at 630 nm. Thus we derive for B_{01} at 630 nm a value of 2.1×10^{-3} s^{-1} J^{-1} m^2.

The triplet quenching constants, Q (kmol^{-1} m^3 s^{-1}), of several different porphyrins have been measured *in vitro* by Bonnet *et al* (1983). For HP they report a value of 1.5×10^9. Parker and Stanbro (1984) report a quenching rate, QM_0, of 4.2×10^5 s^{-1} for HpD in air saturated water, resulting in a triplet decay time, τ_0, of 2.3×10^6 s. Using an oxygen concentration of 3×10^4 kmol m^{-3} for air saturated water, we can derive a value for Q of 1.4×10^9, yielding a perfect match with the result of Bonnet *et al* (1983).

The triplet decay rates of HP in the absence of quenching, k_{20}, reported by Bonnet *et al* (1983) are equal to 4×10^4 (s^{-1}). Thus, when $M_0 = 0$ the triplet lifetime $\tau_0 = 2.5 \times 10^5$ s.

3.2. Oxygen

The initial oxygen concentration, M_{00}, will be based on 100% oxygenation, i.e. $M_{00} = 3 \times 10^{-4}$ kmol m^{-3}, which is the oxygen concentration in air saturated water.

The oxygen supply term, S, from (7*a*) is very difficult to quantify. It is a function of local and systemic perfusion parameters and of local oxygen diffusivity, which may all be different for different tissues and which may change in time due to the PDT. In the first part of our calculations we assume that the oxygen supply term S is large enough to compensate for the consumed oxygen on a 'long'-term basis. Thus for the case of CW excitation we take

$$M_0(t) = M_{00} \qquad \text{(CW excitation)}. \tag{15}$$

The oxygen transport trough tissue is a relatively slow process that depends on diffusion. For the case of pulsed excitation we will assume the oxygen transport to be too slow to contribute during the short time the excitation pulse is causing population changes, i.e. $S = 0$. In the much longer period after the pulse we assume the oxygen ground state concentration to be restored to its initial value:

$$M_0(\vartheta = 0) = M_{00} \qquad \text{(pulsed excitation)}. \tag{16}$$

The lifetime of singlet oxygen, τ_Δ, has been measured by several investigators (Badger *et al* 1965, Gorman and Rodgers 1978, Parker and Stanbro 1984). Our model comprises three competing pathways of singlet oxygen depopulation: luminescence, α_{10}, non-radiative decay to the ground state, κ_{10}, and chemical reactions, κ_{12}. In D_2O values of $\tau_\Delta = 2.2 \times 10^{-4}$ s have been reported, in alcohol τ_Δ decreases to 3×10^{-5} s and in H_2O even to 3×10^{-6} s (Gorman and Rodgers 1978, Redmond *et al* 1987). This strong variation with the environment is related to the fact that this decay is collision induced (Badger *et al* 1965). A similar environmental dependence can be expected for the rate κ_{12}. Foster *et al* (1991) argue that κ_{12} depends strongly on the concentration of singlet oxygen receptors. Separate values of the different parameters are not available. For our calculations it is of particular importance

to estimate what fraction of singlet oxygen is removed from the system; this, according to our model, is the key parameter for determination the photodynamic damage.

Luminescence lifetimes measured (1265 nm) in a cell suspension by Firey *et al* (1988) suggest that in a biological environment τ_Δ is much smaller than the 3×10^6 s measured in pure H_2O, namely less than 0.6×10^{-6} s. Foster *et al* (1991) state that this suggests that the number of singlet oxygen receptors is much larger *in vivo* than in pure H_2O, increasing the *in vivo* value of κ_{12}. This suggests that *in vivo* $\kappa_{12} \gg \alpha_{10}$. This appears to be in contrast to singlet oxygen luminescence measurements at 1272 nm performed *in vivo* in tumour bearing mice during PDT by Parker (1987). In the latter paper, the experimental results were fitted with $\tau_\Delta = 3.2 \times 10^{-6}$ s and a sensitizer triplet lifetime τ_t of 9.6×10^{-6} s. Parker's analysis, however, indicates that a whole range of combinations of values for τ_Δ and τ_t could fit the data accurately. In fact, choosing the much shorter singlet oxygen lifetime reasoned above, i.e. $\tau_\Delta < 10^{-6}$ s, would lead to $\tau_t = 1.2 \times 10^{-5}$ s. Thus, we feel confident to assume that $\kappa_{12} \gg \alpha_{10}$ *in vivo* and take $\kappa_{12} = 1/\tau_\Delta = 10^6$ s^{-1} whereas the individual values of α_{10} and κ_{10} are not important.

3.3. Fluence rates

To avoid thermal effects, the average incident fluence rate I_0 should be kept below a damage threshold. For CW excitation a value of $I_0 = 1500$ W m^{-2} is a commonly used upper limit in PDT and consequently $B_{01} I_0 \ll 1/\tau_0$. Damage thresholds for pulsed lasers at 630 nm are not available. The closest wavelength at which such information is available is 577 nm, a wavelength extensively studied for treatment of portwine stains. The thresholds for inducing purpura on normal caucasian skin reported by Garden *et al* (1986) vary from 1.5×10^4 W m^{-2} at 10^{-6} s pulse duration to 2.5×10^4 W m^{-2} at 10^{-4} s pulse duration. At 630 nm the damage threshold is most likely to be higher because of lower absorption at that wavelength. At 4.8×10^{10} W m^{-2} fluence rate the excitation rate is equal to the de-excitation rate: $B_{01} I_p = 1/\tau_f$. If we stay well below this fluence rate, i.e. $I_p \ll 1/B_{01}\tau_f$, the population of the singlet excited state will not become very large. Once a molecule is excited, it 'immediately' moves to either the ground state or the triplet state, long before any subsequent excitation event takes place. When we look at the response of the populations on a time scale much longer than τ_f, we are interested in the average population of level 1 rather than its rapid variations and take $\mathrm{d}N_1/\mathrm{d}t$ equal to zero. Consequently, N_1 can be eliminated from the equations, reducing (4) to a two-state problem:

$$\mathrm{d}N_0/\mathrm{d}t = -N_0 \Phi_t B_{01} I_0 + N_2(k_{20} + Q M_0) \tag{17a}$$

$$\mathrm{d}N_2/\mathrm{d}t = -\mathrm{d}N_0/\mathrm{d}t. \tag{17b}$$

Earlier (10) we assumed total relaxation of all states before the next pulse arrives. This is the case when $T_r - T_p \gg \tau_0$. This requires $T_r - T_p$ to be larger than 10^{-5} s and consequently f to be below 10^5 Hz for reasonable oxygenation levels.

4. Results

4.1. Solutions for a constant oxygen concentration

In the case where the oxygen concentration is constant, (17) can be solved analytically. We take $M_0(t) = M_{00}$ throughout the exposure, which reflects the situation where the oxygen supply is constant.

4.1.1. CW excitation. With initial conditions from (7) we derive the solution

$$N_0(t) = N_{00}(1 - \tau_0\Phi_t B_{01} I_0(1 - \mathrm{e}^{-t/\tau_0})) \tag{18a}$$

$$N_2(t) = N_{00}\tau_0\Phi_t B_{01} I_0(1 - \mathrm{e}^{-t/\tau_0}). \tag{18b}$$

A steady state will be reached within a time of the order of τ_0 which can be considered 'immediate' on a CW time scale. For these steady values, $\underline{N}_{0,CW}$ and $\underline{N}_{2,CW}$, we derive

$$\underline{N}_{0,CW} = N_{00}(1 - \tau_0\Phi_t B_{01} I_0) \tag{19a}$$

$$\underline{N}_{2,CW} = N_{00}\tau_0\Phi_t B_{01} I_0. \tag{19b}$$

With this result, and using (12), we can derive for the photodynamic damage rate of CW light at equilibrium

$$\mathrm{d}\underline{\Omega}_{CW}/\mathrm{d}t = \varepsilon \underline{M}_{1,CW}\kappa_{12} = \varepsilon M_0 Q \underline{N}_{2,CW} = \varepsilon M_{00} Q N_{00}\tau_0\Phi_t B_{01} I_0. \tag{20}$$

4.1.2. Pulsed excitation. We have assumed that the time between pulses is large enough for total relaxation of all excited states to occur. For each individual pulse the populations during and after the pulse will vary identically for each consecutive pulse. Using the initial conditions (9) and (10), the analytical solution during the pulse will be similar to the CW solution: during the pulse, $0 > \vartheta > T_p$

$$N_0(\vartheta) = N_{00}(1 - [\tau_0\Phi_t B_{01} I_p/(\tau_0\Phi_t B_{01} I_p + 1)](1 - \mathrm{e}^{-\vartheta/\tau_p})) \tag{21a}$$

$$N_2(\vartheta) = N_{00}[\tau_0\Phi_t B_{01} I_p/(\tau_0\Phi_t B_{01} I_p + 1)](1 - \mathrm{e}^{-\vartheta/\tau_p}) \tag{21b}$$

where τ_p is given by

$$\tau_p = \tau_0/(\tau_0\Phi_t B_{01} I_p + 1) \tag{22}$$

and between pulses, $T_p > \vartheta > T_r$, the excitation fluence is zero and all states relaxate to their initial populations:

$$N_0(\vartheta) = N_{00} - N_2(T_p)\,\mathrm{e}^{-(\vartheta - T_p)/\tau_0} \tag{23a}$$

$$N_2(\vartheta) = N_2(T_p)\,\mathrm{e}^{-(\vartheta - T_p)/\tau_0}. \tag{23b}$$

The photodynamic damage per pulse cycle now becomes

$$\int_{\vartheta=0}^{\vartheta=T_r} \frac{\mathrm{d}\Omega_{pulsed}}{\mathrm{d}t}\,\mathrm{d}\vartheta = \varepsilon M_{00} Q N_{00} \frac{\tau_0\Phi_t B_{01} I_p}{\tau_0\Phi_t B_{01} I_p + 1} \times \left(T_p + \tau_0\left(\frac{\tau_0\Phi_t B_{01} I_p}{\tau_0\Phi_t B_{01} I_p + 1}\right)(1 - \mathrm{e}^{-T_p/\tau_p})\right). \tag{24}$$

The relative effectiveness of pulsed light, χ, can now be expressed as

$$\chi = \frac{1}{B_{01} I_p \Phi_t \tau_0 + 1}\{1 + (\tau_0/T_p)(B_{01} I_p \Phi_t \tau_0/(B_{01} I_p \Phi_t \tau_0 + 1))(1 - \mathrm{e}^{-T_p(B_{01} I_p \Phi_t \tau_0 + 1)/\tau_0})\}. \tag{25}$$

Note that by using the equilibrium solution for CW excitation and taking M_0 as constant for pulsed excitation, χ has become independent of time.

Values for χ as a function of the peak fluence rate I_p for different laser pulse durations are shown in figure 4. For large pulse durations the relative effectiveness starts to go down at values of I_p equal to $1/B_{01}\Phi_t\tau_0$ or 4×10^8 W m^{-2}. For shorter pulse durations this effect occurs at higher fluence rates. The saturation fluence rate I_{sat}, defined as the fluence rate at which χ (24) has dropped to 1/e, is depicted in figure 5 as a function of the pulse duration.

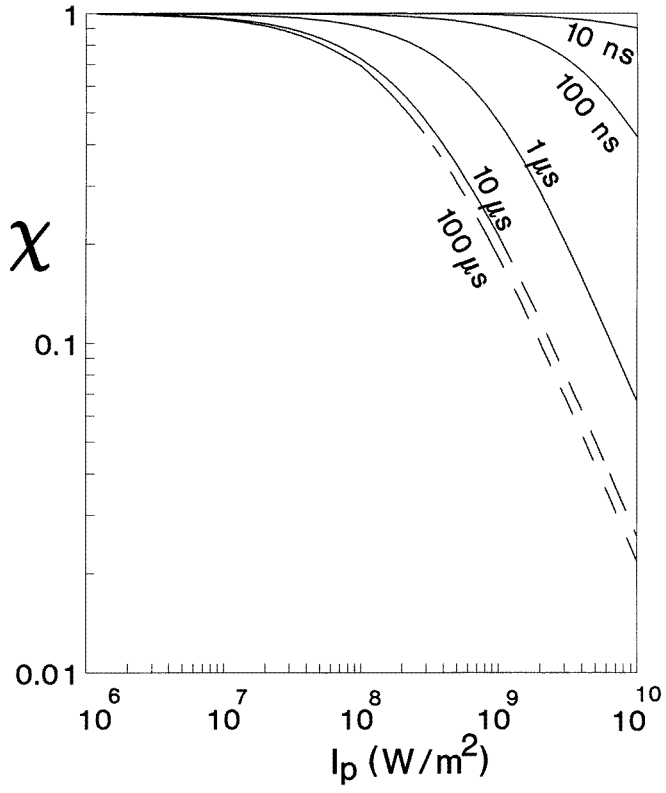

Figure 4. The relative effectiveness, χ, of pulsed light for PDT for different pulse durations as a function of the fluence rate. The dashed lines refer to delivered pulse energies larger than the purpura threshold at 577 (Garden *et al* 1986).

4.2. Oxygen depletion

The derivation of (25) was based on the assumption that the oxygen concentration is constant and therefore may have limited applicability. However, in the case where substantial oxygen depletion takes place on a much longer time scale than the excitation and de-excitation of the different states we can treat the population of the oxygen ground state $M_0(t)$ as a constant, even though it is slowly changing. In other words if we can prove that the relative change in the concentration of ground state oxygen molecules per pulse is small, then (25) is valid for realistic PDT. The change in the ground state oxygen concentration during one pulse cycle, ΔM_0, is calculated by integrating the quenching rate in time:

$$\Delta M_0 = \int_{\vartheta=0}^{\vartheta=T_r} M_0(t)\, Q N_2(t)\, \mathrm{d}t. \tag{26}$$

As we know that M_0 will only go down during the pulse we can write

$$\int_{\vartheta=0}^{\vartheta=T_r} M_0(t)\, Q N_2(t)\, \mathrm{d}t \leqslant M_0(\vartheta = 0) Q \int_{\vartheta_0}^{\vartheta=T_r} N_2(t)\, \mathrm{d}t \tag{27}$$

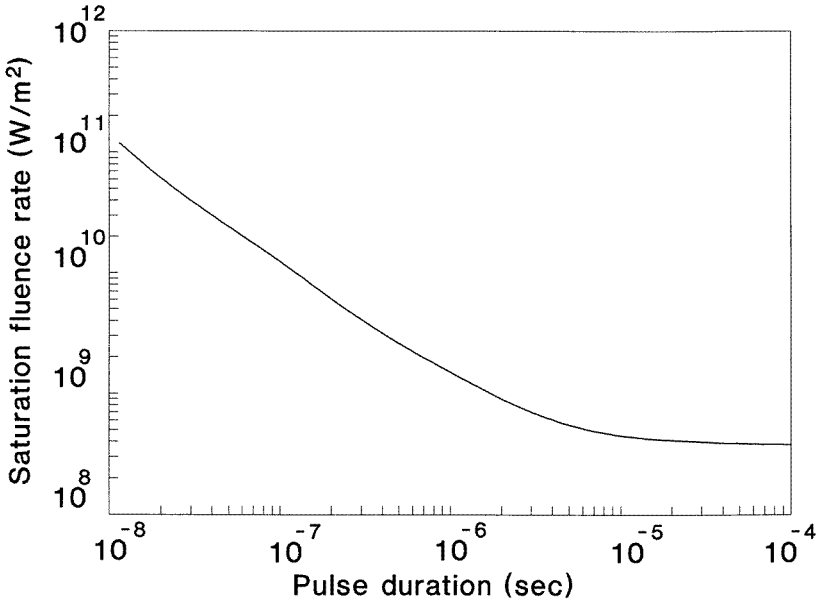

Figure 5. The saturation fluence rate as a function of the pulse duration. The saturation fluence rate is defined as the fluence rate at which the effectiveness χ is equal to 1/e.

and hence

$$\Delta M_0/M_0 \leqslant QN_{00}[B_{01}I_p\Phi_t\tau_0/(B_{01}I_p\Phi_t\tau_0+1)](T_p+\tau_0[B_{01}I_p\Phi_t\tau_0/(B_{01}I_p\Phi_t\tau_0+1)] \times(1-\mathrm{e}^{-T_p(B_{01}I_p\Phi_t\tau_0+1)/\tau_0})). \tag{28}$$

Figure 6 shows the relative change in oxygen concentration calculated using (36), the numerical values mentioned earlier and a porphyrin concentration of 2.5 μg ml^{-1}. It shows that for most realistic cases the amount of oxygen consumed per pulse is less than a few per cent of the initial oxygen concentration. The approach of assuming the oxygen concentration constant during the pulse is thus a reasonable one. However, this also indicates that after multiple pulses a significant oxygen depletion will have occurred and the therapeutic effect will be determined strongly by the unknown oxygen supply term S. This, however, will be the case for pulsed excitation as well as for CW excitation. The more effective CW source will produce more singlet oxygen and will thus consume more oxygen than a pulsed source. In the case where the process is completely limited by the oxygen supply, the effectiveness of any pulsed source will, obviously, become equal to unity.

4.3. Clinical lasers

To evaluate the Cu vapour pumped dye laser (Cu dye), the frequency doubled Nd:YAG laser pumped dye laser (KTP dye) and the flashlamp pumped dye laser we calculated the relative effectiveness for pulse durations of 30 ns, 500 ns and 10 μs as a function of the repetition frequency necessary to produce an average fluence rate of 1500 W m^{-2}. The results, shown in figure 7, indicate that both Cu dye and the KTP dye produce an effect identical to that of a CW laser. The effectiveness of a flashlamp pumped dye laser strongly depends on the pulse repetition frequency of the laser.

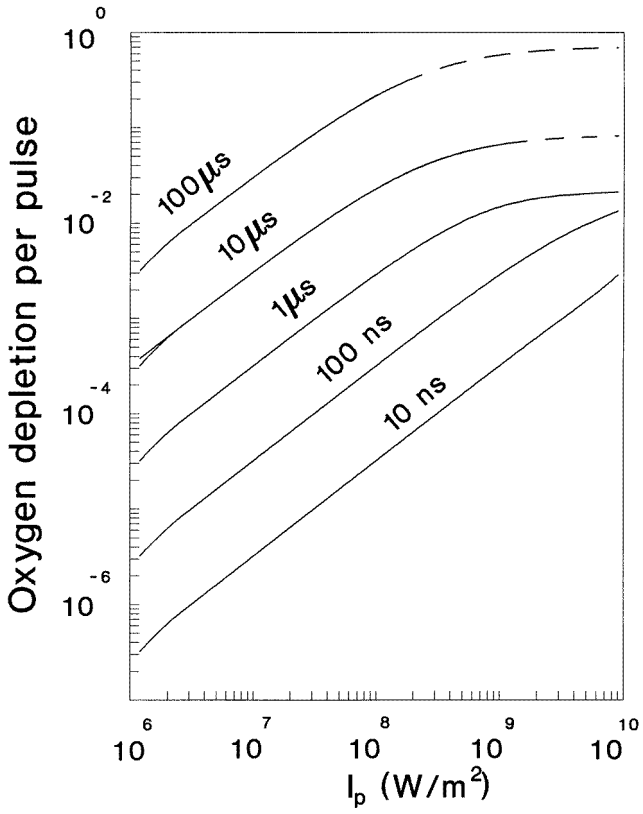

Figure 6. The oxygen depletion per pulse for different pulse durations as a function of the fluence rate. The oxygen depletion is expressed as the fraction of the available oxygen consumed per pulse cycle.

5. Discussion

5.1. The accuracy of the numbers

The data used here were derived from a large number of different studies by different investigators, and yet give a very consistent picture. It is stressed, however, that the concept presented here does not depend on the exact values of the data used. In fact, the result suggest that the parameter of main interest is the triplet decay rate τ_t.

5.2. The effect of a fluence rate distribution

In our analysis we calculated the effectiveness as a function of the fluence rate. In a scattering and absorbing medium such as biologic tissue the fluence rate is not constant, but spatially dependent. As a consequence the effectiveness also becomes spatially dependent; $\chi(r)$. As a consequence χ as defined by equation (25) is actually a local effectiveness.

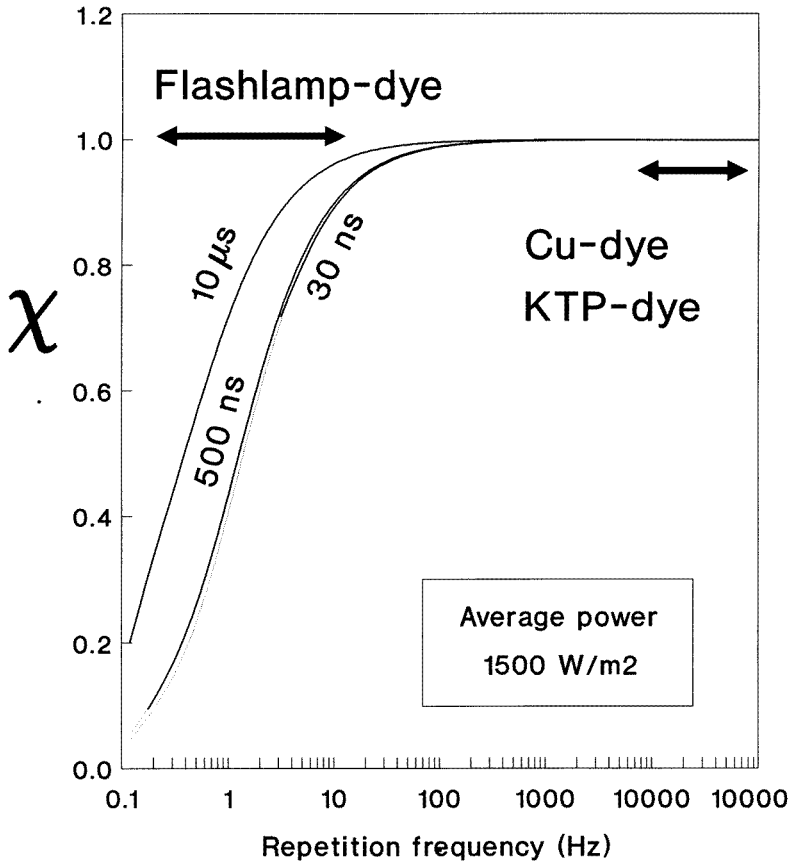

Figure 7. The relative effectiveness as a function of the repetition frequency for three different pulse durations. The results indicate that the Cu dye and the KTP dye lasers, operating at repetition frequencies of 10 kHz or more, have an effectiveness of unity, i.e. identical to CW. For the pulse dye laser, operating at pulse durations between 5×10^{-7} and 10^{-5} s, the effectiveness strongly depends on the repetition frequency.

5.3. The benefit of saturation excitation in PDT

Saturation decreases the photodynamic effectiveness by limiting the photodynamic damage per unit time, Ω_p, to a maximum value. Although this could be considered a disadvantage over CW excitation, as it will induce an important increase of the total treatment time, the advantage of saturation is that the photodynamic effect is only dependent on the local concentration of the photosensitizer, N_{00}, and not on the local fluence rate. Therefore, administering the superficial fluence rate of 10^{10} Wm^{-2}, which is equal to 25 times the saturation fluence rate $1/B_{01}\tau_0$, saturation would occur over a range of $\ln(25) \approx 3$ times the optical penetration depth. Hence, over this whole range the photodynamic effect would only be proportional to the photosensitizer concentration N_{00}, enabling an optimal therapeutic use of the tumour selectivity of the photosensitizer. Whether this approach is feasible with HpD is presently not known. It is possible that, due to the much lower efficacy at saturating fluence levels, photobleaching would prevent administration of a photodynamic dose sufficient for complete tumour kill. However, with more stable and more effective photosensitizers such as mTHPC, such a scheme might be feasible.

5.4. Photobleaching

Photobleaching, the breakdown of the photosensitizer as a result from the exposure to light, has been explicitly omitted from the model because not much is known about the process of photobleaching usng pulsed excitation. Photobleaching as it occurs with CW excitation is most likely a linear process: a constant fraction of all excitations lead, directly or indirectly, to destruction of the photosensitizer molecule, independent of the peak power used. For pulsed excitation, multi-step excitations are more likely to occur, resulting in a higher bleaching rate for higher peak powers, being a non-linear process. Neither details on the mechanisms to enable design of a mathemaatical model, nor numerical data to feed into the model, are presently available. However, for every clinically useful photosensitizer it is a fact that photobeaching is a slow process with respect to the processes modelled in the present paper. Therefore, the two effects can be modelled separately.

6. Conclusions

The effectiveness of pulsed excitation in PDT is identical to that of CW excitation for fluence rates below 4×10^8 W m^{-2}. Above this threshold the effectiveness drops significantly. In practice this effect can only occur with pulsed lasers with high pulse energy and low repetition frequency. The commonly used dye lasers pumped by either a Cu vapour laser or a frequency doubled Nd:YAG laser have a PDT effectiveness identical to that of a CW source of the same wavelength and the same average fluence rate.

References

Badger R M, Wright A C and Whitlock R F 1965 Absolute intensities of the discrete and continuous absorption bands of oxygen gas at 1.26 and 1.065 μm and the radiative lifetime of the singlet state of oxygen *J. Chem. Phys.* **43** 4345–50

Bonnet R, Lambert C, Land E J, Scourides P A, Sinclair R S and Truscott T G 1983 The triplet and radical species of hematoporphyrin and some of its radical species *Photochem. Photobiol.* **38** 1–8

Ferrario A, Rucker N, Ryter S W, Doiron D R and Gomer C J 1991 Direct comparison of *in vitro* and *in vivo* Photofrin II mediated photosensitization using a pulsed KTP pumped dye laser and a continuous wave argon ion pumped dye laser *Lasers Surg. Med.* **11** 404–10

Firey P A, Jones T W, Jori G and Rodgers M A J 1988 Photoexcitation of zinc phthalocyanin mouse myeloma cells: the observation of triplet states but not singlet oxygen *Photochem. Photobiol.* **48** 357–60

Foster T H, Murant R S, Bryant R G, Knox R S, Gibson S L and Hilf R 1991 Oxygen consumption and diffusion effects in photodynamci therapy *Radiat. Res.* **126** 296–303

Garden J M, Tan O T, Kerschmann R, Boil J, Furomoto H, Anderson R R and Parrish J A 1986 Effect of laser pulse duration on selected vascular injury *J. Invest. Dermatol.* **87** 653–7

Gorman A A and Rodgers M A J 1978 Life time and reactivity of singlet oxygen in an aqueous micellar system. A pulsed nitrogen laser study *Chem. Phys. Lett.* **55** 52–4

Hasan T 1991 Multiphoton effects *Proc. SPIE Conf. on Laser–Tissue Interaction II* (Bellingham: SPIE) pp 70–6

Kaye A H, Morstyn G and Brownbill D 1987 Adjuvant high-dose photoirradiation therapy in the treatment of cerebral glioma: a phase 1–2 study *J. Neurosurg.* **67** 500–5

Kozlov A A, Lobko V V, Matveetz Y A, Nikogosian D N and Lethokov V S 1987 Decomposition of thimine sensitized by hematoporphyrin and its derivative at one and two step laser excitation *Lasers Life Sci.* **1** 28–37

Laplant M, Parker J, Stewart B, Waner M and Straight R C 1987 Comparison of the optical transmission properties of pulsed and continuous wave light in biological tissue *Lasers Surg. Med.* **7** 336–8

Moan J and Sommer S 1981 Fluorescence and absorption properties of the components of hematoporphyrin derivative *Photobiochem. Photobiophys.* **3** 93–103

Panjehpur M, Overholt B F, DeNovo R C, Petersen M G and Sneed R E 1993 Comparitive study between pulsed and continuous wave lasers for Photofrin photodynamic therapy *Lasers Surg. Med.* **13** 296–304

Parker J G 1987 Optical monitoring of singlet oxygen generation during photodynamic treatment of tumors *IEEE Circuits Devices Mag.* 10–21

Parker J G and Stanbro W D 1984 Optical determination of the rates of formation and decay of $^1O_2$ in H_2O, D_2O and other solvents *J. Photochem.* **25** 1–8

Pope A J, Masters J R and MacRobert A J 1990 The photodynamic effect of a pulsed dye laser on human bladder carcinoma cells *in vitro Urol. Res.* **18** 267–70

Rausch R C, Rolfs F, Winkler M R, Kottysch A, Schauer A and Steiner W 1993 Pulsed versus continuous wave excitation mechanisms in photodynamic therapy of differently graded squamous cell carcinomas in tumor-implanted nude mice *Eur. Arch. Otorhinolaryngol.* **50** 82–7

Redmond R W, Heihoff K, Braslavski S E and Truscott T G 1987 Thermal lensing and phosphorescence studies of the quantum yield and life time of singlet molecular oxygen sensitized by hematoporphyrin and related porphyrins in deuterated and non-deuterated ethanols *Photochem. Photobiol.* **45** 209–13

Schneckenburger H, Seidlitz H K and Eberz J 1988 Time-resolved fluorescence in photobiology *J. Photochem. Photobiol.* **B2** 1–19